

Structural and Medium Effects on the Reactions of the Cumyloxyl Radical with Intramolecularly Hydrogen Bonded Phenols. The Interplay Between Hydrogen-Bonding and Acid-Base Interactions on the Hydrogen Atom Transfer Reactivity and Selectivity

Michela Salamone,^{*,†} Riccardo Amorati,[‡] Stefano Menichetti,[§] Caterina Viglianisi,[§] and Massimo Bietti^{*,†}

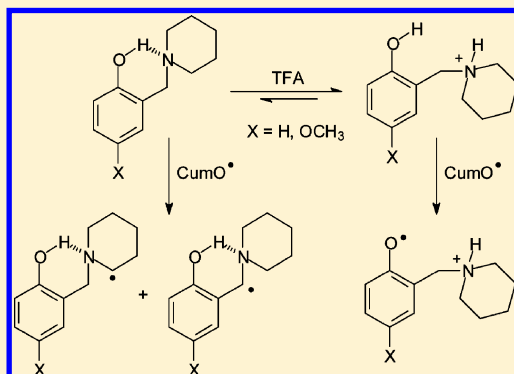
[†]Dipartimento di Scienze e Tecnologie Chimiche, Università "Tor Vergata", Via della Ricerca Scientifica, 1, I-00133 Rome, Italy

[‡]Dipartimento di Chimica "G. Ciamician", Università di Bologna, Via San Giacomo, 11, I-40126 Bologna, Italy

[§]Dipartimento di Chimica "U. Schiff", Università di Firenze, Via della Lastruccia, 3-13, I-50019 Sesto Fiorentino, Italy

S Supporting Information

ABSTRACT: A time-resolved kinetic study on the reactions of the cumyloxyl radical (CumO•) with intramolecularly hydrogen bonded 2-(1-piperidinylmethyl)phenol (**1**) and 4-methoxy-2-(1-piperidinylmethyl)phenol (**2**) and with 4-methoxy-3-(1-piperidinylmethyl)phenol (**3**) has been carried out. In acetonitrile, intramolecular hydrogen bonding protects the phenolic O–H of **1** and **2** from attack by CumO• and hydrogen atom transfer (HAT) exclusively occurs from the C–H bonds that are α to the piperidine nitrogen (α -C–H bonds). With **3** HAT from both the phenolic O–H and the α -C–H bonds is observed. In the presence of TFA or $\text{Mg}(\text{ClO}_4)_2$, protonation or Mg^{2+} complexation of the piperidine nitrogen removes the intramolecular hydrogen bond in **1** and **2** and strongly deactivates the α -C–H bonds of the three substrates. Under these conditions, HAT to CumO• exclusively occurs from the phenolic O–H group of **1**–**3**. These results clearly show that in these systems the interplay between intramolecular hydrogen bonding and Brønsted and Lewis acid–base interactions can drastically influence both the HAT reactivity and selectivity. The possible implications of these findings are discussed in the framework of the important role played by tyrosyl radicals in biological systems.



INTRODUCTION

Proton-coupled electron transfer (PCET) reactions, broadly described as reactions in which both electrons and protons are transferred, are attracting increasing interest, as they are involved in a variety of important chemical and biological processes.^{1,2} Relevant examples include the electron transfer activation of small molecules (O_2 , H_2O , CO_2), nitrogen fixation, hydrocarbon oxidation, and enzymatic reactions such as those catalyzed by photosystem II (PSII), class I ribonucleotide reductase, DNA photolyase, and other systems.

PCET reactions where proton and electron transfers involve different sites and occur in a single kinetic step have been named separated concerted proton–electron transfer (CPET) or, alternatively, multiple site electron–proton transfer (MS-EPT) reactions,¹ as opposed to reactions that occur through sequential electron–proton transfer (ET-PT) and proton–electron transfer (PT-ET) pathways. Hydrogen atom transfer (HAT) is instead described as a PCET reaction where the proton and electron are transferred from one site to another in a single kinetic step,^{1,3} typical examples being represented by the reactions of free radicals (X^\bullet) with hydrogen atom donor substrates S–H (eq 1).



In keeping with the role played by hydrogen-bonded tyrosine residues in CPET reactions occurring in redox enzymes such as PSII,⁴ where photo-oxidation of these residues has been shown to be coupled to the transfer of their phenolic protons to the hydrogen bond accepting histidine residues, and in order to provide a fundamental understanding of the key parameters that govern these processes, a variety of intramolecularly hydrogen bonded phenols have been employed as mechanistic probes and their reactivity toward one-electron oxidants has been thoroughly investigated.^{5–8} Very limited information is instead available on the HAT reactivity of intramolecularly hydrogen bonded phenols.

Recently, in order to obtain information in this respect, some of us have carried out a kinetic study of the reactions of alkylperoxyl (ROO^\bullet) and 2,2-diphenyl-1-picrylhydrazyl (dpph^\bullet) radicals with phenols bearing pendant piperidine bases in the *ortho* and *meta* positions (see structures **2** and **3** in

Received: April 28, 2014

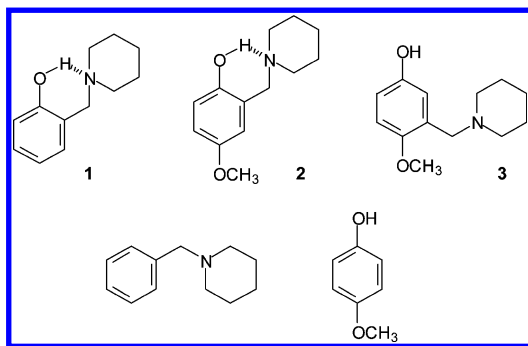
Published: June 3, 2014



Chart 1).⁹ Different reactivity patterns have been observed with the two radicals. With ROO^\bullet the kinetic data have been explained on the basis of a HAT mechanism, showing in particular that, when the phenolic O–H group is involved in an intramolecular hydrogen bond with the piperidine nitrogen, greater than 2 orders of magnitude decreases in the HAT rate constant have been measured. With dpph^\bullet a solvent-dependent competition between HAT and ET (PT-ET or MS-EPT) pathways has been observed instead, a behavior that has been explained on the basis of the higher oxidizing power of dpph^\bullet in comparison to alkylperoxyl radicals.

As has been pointed out in this study, the observation that peroxy radicals are ineffective in HAT from intramolecularly hydrogen bonded phenols can be of great importance in biological systems, as it implies that hydrogen bonding between the phenolic O–H group of tyrosines and basic residues in proteins may protect this group from hydrogen abstraction by reactive oxygen species formed during oxidative stress. Following this indication, it seemed particularly interesting to study the reactions of these substrates with a genuine HAT reagent such as the cumyloxyl radical ($\text{PhC}(\text{CH}_3)_2\text{O}^\bullet$, CumO^\bullet). In comparison to peroxy radicals, for which kinetic information is generally obtained through indirect studies, alkoxyl radicals are known to display a significantly higher HAT reactivity,^{10,11} and CumO^\bullet is characterized by an absorption band in the visible region of the spectrum that makes possible the direct measurement of its reactivity by time-resolved techniques.^{12,13} In addition, this radical can be easily generated from the parent dicumyl peroxide by UV photolysis and is characterized by a relatively low redox potential.¹⁴ Taken together, these features make CumO^\bullet a convenient probe for the study of the HAT reactivity of intramolecularly hydrogen bonded phenols. Along this line, we have carried out a detailed time-resolved spectroscopic and kinetic study of the reactions of CumO^\bullet with phenols 1 and 2, characterized by the presence of a pendant piperidine base in the *ortho* position, whose structures are displayed in Chart 1. As a matter of comparison, the reactions of CumO^\bullet with phenol 3, *N*-benzylpiperidine, and 4-methoxyphenol have been also investigated.

Chart 1

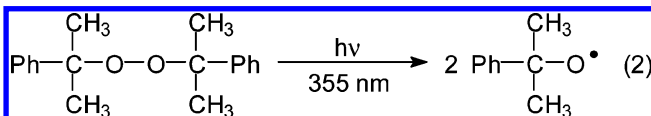


HAT from both phenolic O–H groups^{11b} and the $\alpha\text{-C-H}$ bonds of alkylamines¹⁵ to CumO^\bullet is well established, and accordingly the study of its reactions with phenols 1–3 can provide, in addition to information on the possible protection of the O–H group through intramolecular O–H...N hydrogen bonding mentioned above, useful information on the effect of this interaction on the $\alpha\text{-C-H}$ reactivity. The presence of the piperidine basic center also allows us to probe the effect of Brønsted and Lewis acids on these processes,^{16,17}

in order to understand if, in the reactions with CumO^\bullet , acid–base interactions can influence both the HAT reactivity and selectivity. For this purpose the effects of trifluoroacetic acid (TFA) on the reactions of CumO^\bullet with phenols 1–3 and *N*-benzylpiperidine and of $\text{Mg}(\text{ClO}_4)_2$ on the reactions of CumO^\bullet with phenols 2 and 3 and *N*-benzylpiperidine have been also investigated.

RESULTS AND DISCUSSION

CumO^\bullet has been generated by 355 nm laser flash photolysis (LFP) of argon or oxygen-saturated acetonitrile solutions ($T = 25^\circ\text{C}$) containing 1.0 M dicumyl peroxide, as described in eq 2.



Under these conditions CumO^\bullet is characterized by an absorption band centered at 485 nm^{12,13} and, in the absence of hydrogen atom donor substrates, undergoes C-CH_3 β -scission as the main pathway.^{12,18}

Reactions in Acetonitrile. The reactions of CumO^\bullet with the compounds depicted in Chart 1 have been studied by LFP. The time-resolved spectra observed after reaction of CumO^\bullet with 2-(1-piperidinylmethyl)phenol (1) in an argon-saturated acetonitrile solution are displayed in Figure 1.

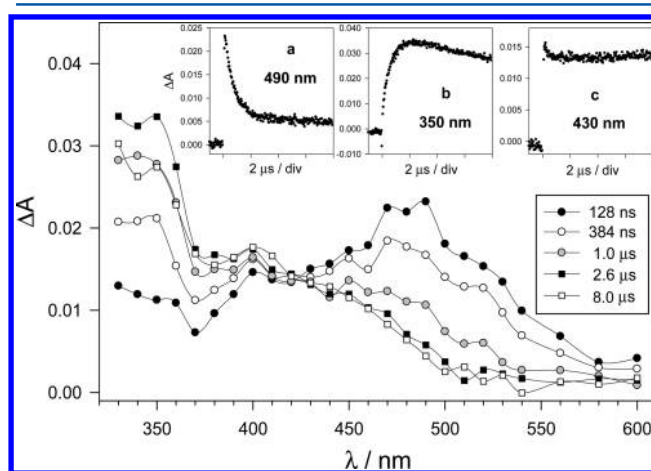


Figure 1. Time-resolved absorption spectra observed after 355 nm LFP of an argon-saturated MeCN solution ($T = 25^\circ\text{C}$) containing dicumyl peroxide (1.0 M) and 2-(1-piperidinylmethyl) phenol (1; 35 mM) at 128 ns (black circles), 384 ns (white circles), 1.0 μs (gray circles), 2.6 μs (black squares), and 8.0 μs (white squares) after the 8 ns, 10 mJ laser pulse. Insets: (a) decay of the cumyloxyl radical monitored at 490 nm; (b) buildup and consequent decay of absorption monitored at 350 nm; (c) decay of absorption monitored at 430 nm.

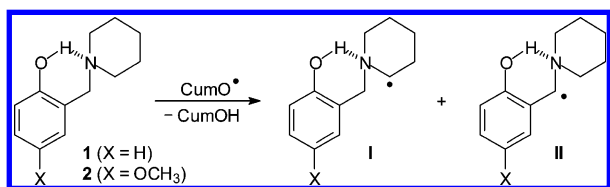
The spectrum recorded 128 ns after the laser pulse is characterized by a broad absorption band centered around 490 nm that, in agreement with literature data,^{12,13} is assigned to CumO^\bullet . The decay of this band (Figure 1, inset a), which is accelerated by the presence of 1, is accompanied by a buildup of absorption between 330 and 420 nm and by a residual absorption between 430 and 500 nm (insets b and c, showing the ΔA vs time profiles monitored at 350 and 430 nm, respectively). An isosbestic point can be identified at 425 nm.

Figure 1 also shows different time evolutions for the UV absorption band centered at 350 nm and the visible absorption band comprised between 390 and 500 nm (insets b and c) where, on the microsecond time scale, a decay of absorption is observed only for the former band, indicating that different species contribute to these absorptions.

A similar behavior has been observed after reaction of CumO[•] with 4-methoxy-2-(1-piperidinylmethyl)phenol (**2**), the spectra for which are displayed in the Supporting Information as Figure S1. The decay of CumO[•] is accompanied by a residual absorption between 390 and 560 nm and by a buildup of absorption between 330 and 370 nm.

The bands observed following decay of CumO[•] in the reactions of both **1** and **2** are assigned to the superimposition of the absorptions of the carbon-centered radicals formed after HAT from the piperidine α -CH₂ and benzylic CH₂ groups (α -C–H bonds thereafter) to CumO[•] as described in Scheme 1

Scheme 1



(radicals **I** and **II**, respectively; X = H, OCH₃), on the basis of a comparison with the time-resolved spectra observed after reaction of CumO[•] with *N*-benzylpiperidine (Figure S2 in the Supporting Information) and with literature data.¹⁹

Support for this assignment is also provided by the time-resolved spectra obtained after reaction of CumO[•] with **1** in an oxygen-saturated acetonitrile solution (Figure S3 in the Supporting Information). In comparison to the corresponding experiment carried out in argon, a significantly weaker absorption at 350 nm is observed, indicating that the species responsible for this absorption reacts with oxygen, as expected

for a carbon-centered radical.²⁰ Under these conditions, the decay of the CumO[•] visible absorption band (Figure S3, inset a) is accompanied by the delayed buildup of an absorption band centered at 430 nm and comprised between 350 and 500 nm (Figure S3, insets b and c, showing the ΔA vs time profiles monitored at 430 and 450 nm, respectively). This band is assigned to the peroxy radicals formed after reaction of radicals **I** and **II** (Scheme 1; X = H) with oxygen, in line with the recent observation that α -aminoalkylperoxy radicals derived from tertiary amines are characterized by absorption bands centered around 400 nm.²¹

Very importantly, under both argon and oxygen, no evidence for the formation of a phenoxyl or a 4-methoxyphenoxyl radical, characterized by two intense absorption bands around 385 and 400 nm and around 340 and 410 nm,^{22,23} respectively, has been obtained (see below), in agreement with the involvement of the phenolic O–H group in an intramolecular hydrogen bond with the piperidine nitrogen. This observation clearly indicates that also with CumO[•] hydrogen bonding protects the O–H group from hydrogen abstraction, despite the significantly higher HAT reactivity displayed by alkoxy radicals in comparison to peroxy radicals,^{10,11} supporting the hypothesis that in these intramolecular hydrogen-bonded phenols HAT exclusively occurs from the α -C–H bonds.

The time-resolved spectra observed after reaction of CumO[•] with 4-methoxy-3-(1-piperidinylmethyl)phenol (**3**) in an argon-saturated acetonitrile solution are displayed in Figure 2A. The decay of CumO[•] (inset a) is accompanied by the formation of a transient species (1.0 μ s, gray circles) characterized by two intense absorption bands at 415 and ≤ 330 nm (insets b and c). An isosbestic point can be identified at 430 nm. These bands are assigned to the 4-methoxy-3-(1-piperidinylmethyl)phenoxyl radical **III**, formed following HAT from the phenolic O–H of **3** to CumO[•] (Scheme 2), on the basis of the comparison with the time-resolved spectrum of the 4-methoxyphenoxyl radical observed after reaction of CumO[•] with 4-methoxyphenol (Figure 2B), characterized by two intense absorption bands at 410 and 340 nm.

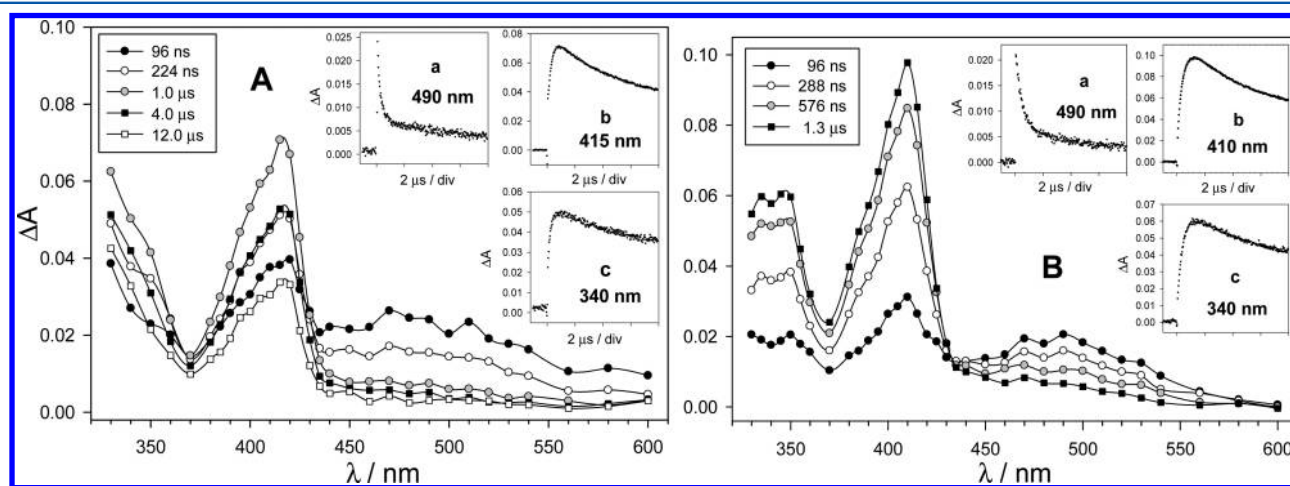
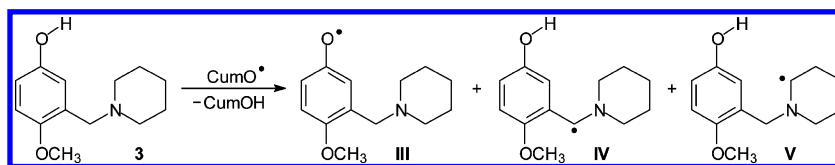


Figure 2. Time-resolved absorption spectra observed after 355 nm LFP of an argon-saturated MeCN solution ($T = 25\text{ }^{\circ}\text{C}$) containing dicumyl peroxide (1.0 M) and (A) 4-methoxy-3-(1-piperidinylmethyl)phenol (**3**; 10 mM) or (B) 4-methoxyphenol (12.1 mM). (A) Spectra recorded at 96 ns (black circles), 224 ns (white circles), 1.0 μ s (gray circles), 4.0 μ s (black squares) and 12 μ s (white squares) after the 8 ns, 10 mJ laser pulse. Insets: (a) decay of the cumyloxyl radical monitored at 490 nm; (b) buildup and consequent decay of absorption monitored at 415 nm; (c) buildup and consequent decay of absorption monitored at 340 nm. (B) Spectra recorded at 96 ns (black circles), 288 ns (white circles), 576 ns (gray circles), and 1.3 μ s (black squares) after the 8 ns, 10 mJ laser pulse. Insets: (a) decay of the cumyloxyl radical monitored at 490 nm; (b) Buildup and consequent decay of absorption monitored at 410 nm; (c) buildup and consequent decay of absorption monitored at 340 nm.

Scheme 2



With phenol **3** the pendant piperidine moiety cannot engage in hydrogen bonding with the O–H group that is free and thus susceptible to attack by CumO•. Unfortunately, due to the strong absorption displayed by phenoxyl radical **III**, from the analysis of Figure 2A no conclusion can be drawn on the possible concomitant formation of radicals **IV** and **V** following HAT from the α -C–H bonds of **3** to CumO•. However, information in this respect is provided by the results of time-resolved kinetic studies on the reaction of CumO• with phenol **3** discussed below.

Time-resolved kinetic studies of the reactions of CumO• with phenols **1–3**, *N*-benzylpiperidine, and 4-methoxyphenol have been carried out by LFP in acetonitrile at $T = 25^\circ\text{C}$, following the decay of the CumO• visible absorption band at 490 nm (540 nm in the reactions with **1** and **2**, in order to limit the contribution of the residual absorption due to radicals **I** and **II**) as a function of the concentration of substrate. From plots of the observed rate constants (k_{obs}) against substrate concentration, excellent linear relationships have been obtained and the second-order rate constant for HAT from these substrates to CumO• (k_{H}) have been derived from the slope of these plots. The k_{obs} vs [substrate] plots for the reactions of CumO• with phenols **1–3**, *N*-benzylpiperidine, and 4-methoxyphenol are displayed in the Supporting Information as Figures S4–S8, respectively. All the kinetic data thus obtained are collected in Table 1, together with indications of the hydrogen atom abstraction site (α -C–H and/or O–H) for the different substrates.

Table 1. Second-Order Rate Constants (k_{H}) for HAT from Different Substrates to the Cumyloxyl Radical (CumO•), Measured in Acetonitrile at $T = 25^\circ\text{C}$

substrate	$k_{\text{H}}/\text{M}^{-1} \text{ s}^{-1}$ ^a	abstraction site
1	1.7×10^7	α -C–H
2	3.4×10^7	α -C–H
3	2.4×10^8	α -C–H and O–H
<i>N</i> -benzylpiperidine	1.3×10^8	α -C–H
4-methoxyphenol	8.3×10^7	O–H

^aMeasured in argon-saturated solution employing 355 nm LFP: [dicumyl peroxide] = 1.0 M. k_{H} values have been determined from the slope of the k_{obs} vs [substrate] plots, where in turn k_{obs} values have been measured following the decay of the CumO• visible absorption band at 490–540 nm. Error $\leq 10\%$.

The following k_{H} values have been measured for the reactions of **1** and **2** with CumO•: $k_{\text{H}} = 1.7 \times 10^7$ and $3.4 \times 10^7 \text{ M}^{-1} \text{ s}^{-1}$, respectively. On the basis of the discussion outlined above, these values refer to HAT from the α -C–H bonds as described in Scheme 1. Comparison between the value measured for **1** and the k_{H} value measured analogously for HAT from *N*-benzylpiperidine to CumO• ($k_{\text{H}} = 1.3 \times 10^8 \text{ M}^{-1} \text{ s}^{-1}$) shows that intramolecular hydrogen bonding leads to an almost 8-fold decrease in k_{H} . Along this line, the 2-fold increase in k_{H} observed on going from **1** to **2** can be reasonably

explained on the basis of the slightly higher hydrogen bond donor (HBD) ability of phenol in comparison to 4-methoxyphenol (as measured by Abraham's α_2^{H} parameters: 0.60 and 0.57, respectively)²⁴ that results in a decrease in the strength of the intramolecular hydrogen bond on going from **1** to **2**.

The role of intermolecular hydrogen bond interactions on HAT reactions from tertiary alkylamines has been recently investigated, showing that in the reaction of CumO• with triethylamine k_{H} decreases with increasing solvent HBD ability. An almost 6-fold decrease in k_{H} has been measured on going from acetonitrile to MeOH (for which $k_{\text{H}} = 2.19 \times 10^8$ and $3.8 \times 10^7 \text{ M}^{-1} \text{ s}^{-1}$, respectively).²⁵ This behavior has been explained on the basis of the decrease in the degree of overlap between the α -C–H bond and the amine lone pair determined by solvent hydrogen bonding. When HBD solvents engage in hydrogen bonding with the nitrogen center, this interaction decreases the degree of hyperconjugative overlap between the α -C–H σ^* orbital and the lone pair, leading to an increase in the strength of this bond and to a destabilization of the HAT transition state and of the carbon-centered radical formed after abstraction, thus determining a certain extent of deactivation of the α -C–H bonds toward HAT.

On the basis of this picture, a similar explanation can be put forward to account for the decrease in k_{H} observed on going from *N*-benzylpiperidine to **1** (and **2**) where intramolecular hydrogen bonding between the phenolic O–H and the piperidine nitrogen leads to a comparable α -C–H deactivation.

In the reaction of CumO• with phenol **3** a value $k_{\text{H}} = 2.4 \times 10^8 \text{ M}^{-1} \text{ s}^{-1}$ has been obtained. This value is almost three times higher than the value measured for HAT from 4-methoxyphenol to CumO• ($k_{\text{H}} = 8.3 \times 10^7 \text{ M}^{-1} \text{ s}^{-1}$) despite the almost identical O–H BDEs available for these two compounds (81.5 and 81.4 kcal mol^{−1} for **3** and 4-methoxyphenol,⁹ respectively). On the basis of this observation the k_{H} value measured for reaction between CumO• and **3** reasonably reflects the contribution of HAT from both the O–H and α -C–H bonds to give phenoxyl radical **III** and carbon-centered radicals **IV** and **V**, as described in Scheme 2. Support for this hypothesis is also provided by the observation that this value ($k_{\text{H}} = 2.4 \times 10^8 \text{ M}^{-1} \text{ s}^{-1}$) is very close to the sum of the k_{H} values measured under identical experimental conditions for HAT from *N*-benzylpiperidine and 4-methoxyphenol to CumO• ($2.13 \times 10^8 \text{ M}^{-1} \text{ s}^{-1}$).

It is also very interesting to compare the rate constants obtained in this study for reaction of CumO• with phenols **2** and **3** with those measured previously for the corresponding reactions of these substrates with alkylperoxyl (ROO•) and 2,2-diphenyl-1-picrylhydrazyl (dpph•) radicals.⁹ The reactions of ROO• and CumO• can be rationalized on the basis of the HAT mechanism described in Schemes 1 and 2, where however with both substrates a 4-order of magnitude increase in k_{H} is observed on going from the former to the latter radical, in line with the significantly higher HAT reactivity displayed by alkoxyl radicals in comparison to peroxyl radicals.^{10,11} Along this line,

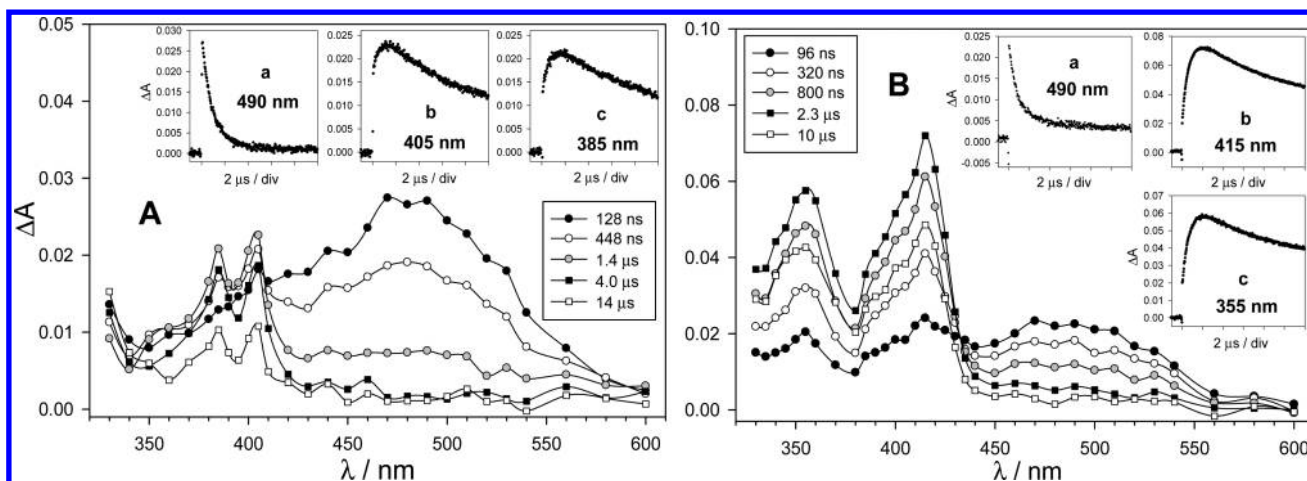


Figure 3. Time-resolved absorption spectra observed after 355 nm LFP of argon-saturated MeCN solutions ($T = 25\text{ }^{\circ}\text{C}$) containing trifluoroacetic acid (TFA), dicumyl peroxide (1.0 M), and (A) 2-(1-piperidinylmethyl)phenol (**1**) or (B) 4-methoxy-2-(1-piperidinylmethyl)phenol (**2**). A: $[\mathbf{1}] = 100\text{ mM}$, $[\text{TFA}] = 112\text{ mM}$, spectra recorded at 128 ns (black circles), 448 ns (white circles), 1.4 μs (gray circles), 4.0 μs (black squares), and 14 μs (white squares) after the 8 ns, 10 mJ laser pulse. Insets: (a) decay of the cumyloxyl radical monitored at 490 nm; (b) buildup and consequent decay of absorption monitored at 405 nm; (c) buildup and consequent decay of absorption monitored at 385 nm. B: $[\mathbf{2}] = 10.8\text{ mM}$, $[\text{TFA}] = 12\text{ mM}$, spectra recorded at 96 ns (black circles), 320 ns (white circles), 800 ns (gray circles), 2.3 μs (black squares), and 10 μs (white squares) after the 8 ns, 10 mJ laser pulse. Insets: (a) decay of the cumyloxyl radical monitored at 490 nm; (b) buildup and consequent decay of absorption monitored at 415 nm; (c) buildup and consequent decay of absorption monitored at 355 nm.

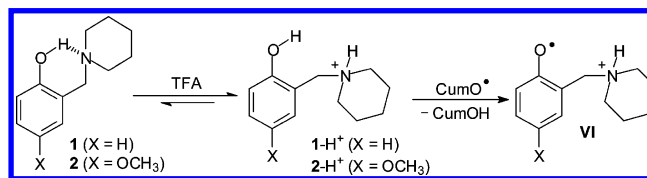
the low rate constant measured for the reaction of ROO^{\bullet} with the intramolecularly hydrogen bonded phenol **2** in acetonitrile solution ($k_{\text{H}} = 2.0 \times 10^3\text{ M}^{-1}\text{ s}^{-1}$) reasonably reflects HAT from the $\alpha\text{-C-H}$ bonds. On the other hand, the PT-ET and MS-EPT pathways described previously for the reactions of dpph^{\bullet} with **2** and **3** are clearly not accessible to CumO^{\bullet} due to the lower oxidizing power of this radical in comparison to dpph^{\bullet} ($E^{\circ} = -0.19$ and 0.23 V/SCE for CumO^{\bullet} and dpph^{\bullet} ,^{9,26,27} respectively).

Reactions in Acetonitrile Containing TFA or $\text{Mg}(\text{ClO}_4)_2$. The effect of TFA and $\text{Mg}(\text{ClO}_4)_2$ has been then investigated. The time-resolved spectra observed after reaction of CumO^{\bullet} with phenols **1** and **2** in argon-saturated acetonitrile solutions containing TFA (at $[\text{substrate}] < [\text{TFA}]$) are displayed in parts A and B of Figure 3, respectively. With both substrates the decay of CumO^{\bullet} is accompanied by the formation of a transient species characterized by two absorption bands at 405 and 385 nm (Figure 3A, gray circles and insets b and c) and 415 and 355 nm (Figure 3B, gray circles and insets b and c). Isosbestic points can be identified between 405 and 410 nm (Figure 3A) and between 430 and 435 nm (Figure 3B).

These bands are very similar to those observed previously for the phenoxyl and 4-methoxyphenoxyl radicals, the former characterized by absorption bands centered at 400 and 385 nm with a shoulder at 360 nm²² and the latter by absorption bands centered at 410 and 340 nm (Figure 2B), and accordingly are assigned to the distonic phenoxyl radical cations **VI**. Formation of **VI** can be explained on the basis of HAT from the free phenolic O–H group of protonated **1** and **2** (1-H^+ and 2-H^+) that in turn are formed by TFA protonation of the piperidine nitrogen as described in Scheme 3 ($X = \text{H}, \text{OCH}_3$).

Figure 3 also shows that as compared to the spectra recorded in acetonitrile (Figure 1 and Figure S1 (Supporting Information)) after addition of TFA the spectrum assigned to the carbon-centered radicals **I** and **II** (Scheme 1) is replaced by the absorption spectra of the distonic phenoxyl radical cation **VI**. This observation is in full agreement with the recently described $\alpha\text{-C-H}$ bond deactivation of alkylamines by

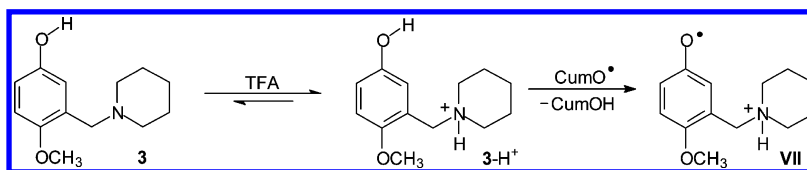
Scheme 3

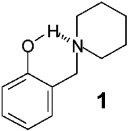
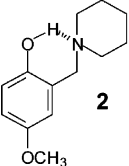
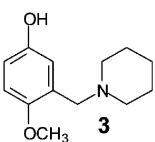
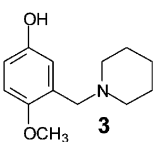
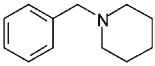
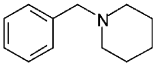
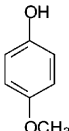


protonation,¹⁶ where the formation of an ammonium ion prevents overlap between the $\alpha\text{-C-H}$ bonds and the nitrogen lone pair and leads to greater than 4 orders of magnitude decreases in HAT reactivity. Most importantly, these findings clearly show that in intramolecularly hydrogen bonded phenols such as **1** and **2** the HAT selectivity can be drastically changed through acid–base interactions. Protonation of the piperidine nitrogen removes the hydrogen bond interaction strongly deactivating the $\alpha\text{-C-H}$ bonds and changing the abstraction site from these bonds (Scheme 1) to the phenolic O–H group (Scheme 3).

A very similar behavior has been observed when the reaction of CumO^{\bullet} with phenol **2** has been studied in the presence of $\text{Mg}(\text{ClO}_4)_2$. The time-resolved spectra thus obtained in an argon-saturated acetonitrile solution containing 10.5 mM **2** and 11.2 mM $\text{Mg}(\text{ClO}_4)_2$ are displayed in the Supporting Information as Figure S9. Also under these conditions the decay of CumO^{\bullet} is accompanied by the formation of a transient species characterized by two intense absorption bands at 415 and 355 nm that is assigned to the 4-methoxyphenoxyl radical having the piperidine nitrogen atom coordinated to the magnesium ion. On the basis of these results it clearly appears that, in addition to protonation, also Mg^{2+} complexation with a Lewis basic center involved in intramolecular hydrogen bonding with the phenolic O–H can be successfully exploited as a tool to control the HAT selectivity. Also, this observation is in full agreement with the recently described strong deactivation toward abstraction from the $\alpha\text{-C-H}$ bonds of alkylamines determined by coordination of the nitrogen center to Mg^{2+} .¹⁷

Scheme 4

Table 2. Second-Order Rate Constants (k_H) for HAT from Different Substrates to the Cumyloxy Radical (CumO[•]), Measured at $T = 25\text{ }^{\circ}\text{C}$

substrate	conditions	$k_H / \text{M}^{-1} \text{s}^{-1} \text{ }^a$	abstraction site
 1	MeCN	1.7×10^7	$\alpha\text{-C-H}$
	TFA 105 mM	3.0×10^6 at $[1] \leq [\text{TFA}]$	O-H
		1.2×10^7 at $[1] > [\text{TFA}]$	$\alpha\text{-C-H}$
 2	MeCN	3.4×10^7	$\alpha\text{-C-H}$
	TFA 20 mM	3.0×10^7 at $[2] \leq [\text{TFA}]$	O-H
		2.5×10^7 at $[2] > [\text{TFA}]$	$\alpha\text{-C-H}$
 3	Mg(ClO ₄) ₂ 15 mM	8.3×10^7 at $[2] \leq [\text{Mg}(\text{ClO}_4)_2]$	O-H
	MeCN	2.4×10^8	$\alpha\text{-C-H}$ and O-H
	TFA 20 mM	3.5×10^7 at $[3] \leq [\text{TFA}]$	O-H
 3	Mg(ClO ₄) ₂ 16 mM	1.9×10^8 at $[3] > [\text{TFA}]$	$\alpha\text{-C-H}$ and O-H
		6.4×10^7 at $[3] \leq [\text{Mg}(\text{ClO}_4)_2]$	O-H
	MeCN	1.3×10^8	$\alpha\text{-C-H}$
	TFA 10 mM	$< 1 \times 10^6$ at $[\text{sub}] \leq [\text{TFA}]$	$\alpha\text{-C-H}$
		1.4×10^8 at $[\text{sub}] > [\text{TFA}]$	$\alpha\text{-C-H}$
	Mg(ClO ₄) ₂ 10 mM	$< 1 \times 10^6$ at $[\text{sub}] \leq 3/2[\text{Mg}(\text{ClO}_4)_2]$	$\alpha\text{-C-H}$
		1.1×10^8 at $[\text{sub}] > 3/2[\text{Mg}(\text{ClO}_4)_2]$	$\alpha\text{-C-H}$
	MeCN	8.3×10^7	O-H

^aMeasured in argon-saturated acetonitrile solution employing 355 nm LFP: [dicumyl peroxide] = 1.0 M. k_H values have been determined from the slope of the k_{obs} vs [substrate] plots, where in turn k_{obs} values have been measured following the decay of the CumO[•] visible absorption band at 490–540 nm. Error $\leq 10\%$.

The time-resolved spectra observed after reaction of CumO[•] with phenol 3 (9.8 mM) in an argon-saturated acetonitrile solution containing 12 mM TFA is displayed in the Supporting Information as Figure S10. The decay of CumO[•] is accompanied by the formation of two intense absorption bands at 410 and 350 nm that are assigned to the dicationic 4-methoxyphenoxy radical cation VII formed following HAT from the phenolic O–H group of protonated 3 (3-H⁺) to CumO[•], as described in Scheme 4. In comparison to the spectrum recorded in acetonitrile (Figure 2), a ≥ 20 nm red shift of the phenoxy radical UV band is observed following nitrogen protonation. Under these conditions, nitrogen protonation strongly deactivates the $\alpha\text{-C-H}$ bonds and HAT from the phenolic O–H now represents the exclusive reaction pathway.

In order to obtain quantitative information on the deactivating effect of TFA and Mg(ClO₄)₂ on the reactions of CumO[•] with phenols 1–3 and with *N*-benzylpiperidine,

time-resolved kinetic studies have been also carried out. The k_H values thus obtained are collected in Table 2 together with the indication of the hydrogen atom abstraction site ($\alpha\text{-C-H}$ and/or O–H) for the different substrates under the experimental conditions employed. For comparison, also included in this table are the k_H values shown in Table 1 for the reactions of CumO[•] with phenols 1–3, *N*-benzylpiperidine, and 4-methoxyphenol in MeCN.

When HAT from 1 to CumO[•] has been studied in an argon-saturated acetonitrile solution containing 105 mM TFA, k_{obs} has been observed to increase linearly with increasing [1] up to [1] = [TFA], leading to a rate constant for HAT $k_{H1} = 3.0 \times 10^6 \text{ M}^{-1} \text{s}^{-1}$ (Figure 4, black circles).

A linear increase in k_{obs} , but with a different slope, has been then observed for [1] > [TFA], from which, in the 105–150 mM [1] range, a value $k_{H2} = 1.2 \times 10^7 \text{ M}^{-1} \text{s}^{-1}$ has been obtained (Figure 4, white circles).

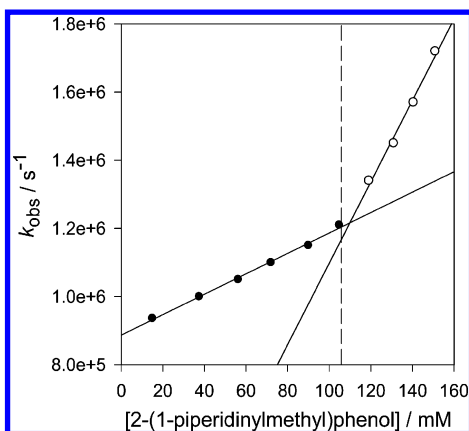


Figure 4. Plots of the observed rate constant (k_{obs}) against concentration of 2-(1-piperidinylmethyl)phenol (**1**) for reaction of the cumyloxyl radical (CumO^\bullet) measured at $T = 25^\circ\text{C}$ in an argon-saturated MeCN solution containing 105 mM trifluoroacetic acid (TFA), by following the decay of CumO^\bullet at 490 nm. From the linear regression analysis: in the 0–105 mM [**1**] range (black circles) $k_{\text{H1}} = 3.00 \times 10^6 \text{ M}^{-1} \text{ s}^{-1}$, $r^2 = 0.9964$; in the 105–150 mM [**1**] range (white circles) $k_{\text{H2}} = 1.19 \times 10^7 \text{ M}^{-1} \text{ s}^{-1}$, $r^2 = 0.9897$. The dashed line indicates the point where [**1**] = [TFA] = 105 mM.

In the reaction of CumO^\bullet with **2** in an argon-saturated acetonitrile solution containing 20 mM TFA, the plot for which is displayed in the Supporting Information as Figure S11, values of $k_{\text{H1}} = 3.0 \times 10^7 \text{ M}^{-1} \text{ s}^{-1}$ and $k_{\text{H2}} = 2.5 \times 10^7 \text{ M}^{-1} \text{ s}^{-1}$ have been obtained for [**2**] \leq [TFA] and [**2**] $>$ [TFA] (in the 20–38 mM [**2**] range), respectively.

The k_{obs} vs [**3**] plots obtained after reaction with CumO^\bullet in an argon-saturated acetonitrile solution containing 19.6 mM TFA are displayed in the Supporting Information as Figure S12. Values of $k_{\text{H1}} = 3.5 \times 10^7 \text{ M}^{-1} \text{ s}^{-1}$ and $k_{\text{H2}} = 1.9 \times 10^8 \text{ M}^{-1} \text{ s}^{-1}$ have been obtained for [**3**] \leq [TFA] and [**3**] $>$ [TFA] (in the 20–30 mM [**3**] range), respectively.

On the basis of the discussion outlined above, at [substrate] \leq [TFA] phenols **1**–**3** only exist in the protonated form ($1\text{-H}^+ \text{--} 3\text{-H}^+$), and accordingly the k_{H1} values reflect HAT from the free phenolic O–H groups of these species to CumO^\bullet as described in Schemes 3 and 4. Comparison between the k_{H1} values thus obtained ($k_{\text{H1}} = 3.0 \times 10^6$, 3.0×10^7 , and $3.5 \times 10^7 \text{ M}^{-1} \text{ s}^{-1}$ for $1\text{-H}^+ \text{--} 3\text{-H}^+$, respectively) and the k_{H} values measured in acetonitrile under analogous experimental conditions for HAT from phenol and 4-methoxyphenol to CumO^\bullet ($k_{\text{H}} = 1.1 \times 10^7 \text{ M}^{-1} \text{ s}^{-1}$ ²² and $8.3 \times 10^7 \text{ M}^{-1} \text{ s}^{-1}$, respectively) shows that the introduction of a protonated 1-piperidinylmethyl ring substituent determines an up to 4-fold decrease in the rate constant for HAT from the phenolic O–H group. This behavior can be reasonably explained on the basis of the electron-withdrawing effect exerted by the ammonium group, as it is well-known that the introduction of EWG ring substituents in phenols leads to an increase in the O–H bond dissociation enthalpy (BDE) and to a corresponding decrease in k_{H} .^{11b,28}

At [substrate] $>$ [TFA] the k_{H2} values measured with **1** and **2** (1.2×10^7 and $2.5 \times 10^7 \text{ M}^{-1} \text{ s}^{-1}$, respectively) reflect instead HAT from the $\alpha\text{-C-H}$ bonds of intramolecularly hydrogen bonded **1** and **2** (Scheme 1), as confirmed by the observation that these values are in both cases very close to the values measured previously for reaction of CumO^\bullet with **1** and **2** in acetonitrile, in the absence of TFA ($k_{\text{H}} = 1.7 \times 10^7$ and $3.4 \times 10^7 \text{ M}^{-1} \text{ s}^{-1}$, respectively; see above). Support for this

hypothesis is also provided by the comparison of the latter k_{H} values with the k_{H1} and k_{H2} values measured for the corresponding reactions of **1** and **2** in the presence of TFA. For [substrate] \leq [TFA] a 1 order of magnitude increase in k_{H1} has been observed on going from $1\text{-H}^+ \text{--} 2\text{-H}^+$ ($k_{\text{H1}} = 3.0 \times 10^6$ and $3.0 \times 10^7 \text{ M}^{-1} \text{ s}^{-1}$, respectively), in full agreement with the activating effect exerted by a methoxy ring substituent on HAT from the phenolic O–H. For [substrate] $>$ [TFA], similar k_{H2} values and almost identical $k_{\text{H2}}/k_{\text{H}}$ ratios (0.71 and 0.74, for **1** and **2**, respectively) have been obtained instead.

For **3**, the measured k_{H2} value at [**3**] $>$ [TFA] ($1.9 \times 10^8 \text{ M}^{-1} \text{ s}^{-1}$) is very similar to the value measured for the corresponding reaction with CumO^\bullet in acetonitrile in the absence of TFA ($k_{\text{H}} = 2.4 \times 10^8 \text{ M}^{-1} \text{ s}^{-1}$), indicating that under these conditions k_{H2} reflects HAT from the $\alpha\text{-C-H}$ and O–H bonds of **3** as described in Scheme 2.

Support for the reactivity patterns observed in the reactions of phenols **1**–**3** after addition of TFA is provided by the results of time-resolved kinetic studies on the reaction between CumO^\bullet and *N*-benzylpiperidine carried out in the presence of TFA, the plots for which are displayed in the Supporting Information as Figure S13. In the presence of 10 mM TFA, no increase in k_{obs} has been observed up to [*N*-benzylpiperidine] = [TFA], providing an upper limit to the rate constant for HAT from *N*-benzylpiperidine to CumO^\bullet as $k_{\text{H}} < 1 \times 10^6 \text{ M}^{-1} \text{ s}^{-1}$. An identical behavior, indicative of stoichiometric protonation of the amine by TFA and of strong $\alpha\text{-C-H}$ deactivation, has been described previously for the reactions between CumO^\bullet and other tertiary alkylamines, where, as mentioned above, greater than 4 orders of magnitude decreases in HAT reactivity have been observed after addition of TFA.¹⁶ For [*N*-benzylpiperidine] $>$ [TFA], a linear increase in k_{obs} with increasing [*N*-benzylpiperidine] has been observed and a rate constant for HAT has been obtained from the slope of this plot as $k_{\text{H}} = 1.4 \times 10^8 \text{ M}^{-1} \text{ s}^{-1}$. This value is very close to the value measured previously for the reaction of CumO^\bullet with *N*-benzylpiperidine in acetonitrile, in the absence of TFA ($k_{\text{H}} = 1.3 \times 10^8 \text{ M}^{-1} \text{ s}^{-1}$, see above and Figure S7 (Supporting Information)), indicating that the measured rate constant now reflects HAT from the $\alpha\text{-C-H}$ bonds of the nonprotonated amine.

The effect of $\text{Mg}(\text{ClO}_4)_2$ on the reactions of CumO^\bullet with *N*-benzylpiperidine and with phenols **2** and **3** has been also investigated. The k_{obs} vs [substrate] plots thus obtained are displayed in the Supporting Information as Figures S14–S16. When the reaction between CumO^\bullet and *N*-benzylpiperidine was studied in the presence of 10 mM $\text{Mg}(\text{ClO}_4)_2$ (Figure S14), no increase in k_{obs} was observed up to [*N*-benzylpiperidine] = $3/2[\text{Mg}(\text{ClO}_4)_2]$,²⁹ indicative of the formation of a Lewis acid–base complex between Mg^{2+} and the nitrogen center that strongly deactivates the $\alpha\text{-C-H}$ bonds toward abstraction, in line with the very large decreases in HAT reactivity that have been observed for the reactions between CumO^\bullet and other tertiary alkylamines, after addition of $\text{Mg}(\text{ClO}_4)_2$.¹⁷ In this context, it is important to point out that a very recent computational study has shown that the interaction between Mg^{2+} and the nitrogen lone pair of triethylamine leads to a 5.1 kcal mol^{−1} increase in the $\alpha\text{-C-H}$ BDE and to a greater than 4 order of magnitude decrease in k_{H} .³⁰ For [*N*-benzylpiperidine] $>$ $3/2[\text{Mg}(\text{ClO}_4)_2]$, a linear increase in k_{obs} with increasing [*N*-benzylpiperidine] has been observed and the rate constant for HAT has been obtained from the slope of this plot as $k_{\text{H}} = 1.1 \times 10^8 \text{ M}^{-1} \text{ s}^{-1}$, a value

that is again very close to the value measured previously for the reaction of CumO• with *N*-benzylpiperidine in acetonitrile, in the absence of Mg(ClO₄)₂ ($k_H = 1.3 \times 10^8 \text{ M}^{-1} \text{ s}^{-1}$; see above and Figure S7 (Supporting Information)), indicating that under these conditions the measured rate constant reflects HAT from the α -C–H bonds of the noncomplexed amine.

By taking into account this strong deactivation of the α -C–H bonds determined by Mg²⁺ complexation, the k_H values measured after reaction of CumO• with phenols **2** and **3** in the presence of Mg(ClO₄)₂ at [substrate] \leq [Mg(ClO₄)₂] ($k_H = 8.3 \times 10^7$ and $6.4 \times 10^7 \text{ M}^{-1} \text{ s}^{-1}$; Figures S15 and S16 (Supporting Information), respectively) are assigned to HAT from the free phenolic O–H groups. This is in full agreement with the spectral evidence provided above for the reaction of CumO• with **2** in the presence of Mg(ClO₄)₂ (Figure S9 (Supporting Information)), indicative of the formation of a 4-methoxyphenoxy radical bound to magnesium through the piperidine nitrogen. Very interestingly, the k_H values measured under these conditions are very close to the k_H value measured for HAT from 4-methoxyphenol to CumO• ($k_H = 8.3 \times 10^7 \text{ M}^{-1} \text{ s}^{-1}$) and are 2–3 times higher than the corresponding k_H values measured for HAT from the O–H bonds of 2-H⁺ and 3-H⁺ discussed above. By ruling out HAT from the α -C–H bonds of Mg²⁺-bound **2** and **3**,¹⁹ this behavior may be explained in terms of perchlorate binding to magnesium in the Lewis acid–base complex with the piperidine nitrogen that results in a weaker electron withdrawing effect of this group in comparison to a protonated piperidinylmethyl group.

In conclusion, the results obtained in this study have clearly shown that in the reactions between CumO• and phenols **1**–**3** both the HAT reactivity and selectivity can be drastically influenced by the interplay between intramolecular hydrogen bonding and acid–base interactions. In acetonitrile intramolecular hydrogen bonding with the piperidine nitrogen, which is operative with phenols **1** and **2**, protects the phenolic O–H group from HAT and leads to a certain extent of deactivation of the α -C–H bonds, quantified in the almost 1 order of magnitude decrease in k_H measured on going from **1** to *N*-benzylpiperidine, where the nitrogen atom is not involved in hydrogen bonding. Under these conditions exclusive HAT from the α -C–H bonds of **1** and **2** is observed. With the free phenol **3** HAT occurs from the α -C–H and O–H bonds. Addition of TFA leads to stoichiometric nitrogen protonation that results in the removal of the intramolecular hydrogen bond interaction in 1-H⁺ and 2-H⁺ and in a strong deactivation of the α -C–H bonds of 1-H⁺–3-H⁺. Under these conditions exclusive HAT from the free phenolic O–H group of these substrates occurs. An analogous effect has been observed in the reactions of CumO• with **2** and **3** after addition of Mg(ClO₄)₂ where the α -C–H deactivation determined by a Lewis acid–base interaction between the magnesium ion and the piperidine nitrogen leads in both cases to exclusive HAT from the phenolic O–H, clearly showing that, in addition to protonation, also Mg²⁺ complexation with a Lewis basic center can be successfully exploited as a tool to control the HAT selectivity. Along these lines, the results obtained in this study suggest that, in the reaction between free radicals and phenolic compounds of biological interest, the interplay between hydrogen bonding and both Brønsted and Lewis acid–base interactions can be of crucial importance in modulating the formation of phenoxy radicals. In particular, these findings appear to be of great interest in the framework of the important role played by tyrosyl radicals in a variety of processes. For example, the intermediacy of tyrosyl

radicals has been evidenced in enzymatic redox reactions occurring in systems such as PSII, ribonucleotide reductase, prostaglandin H synthase, and galactose oxidase,^{1,4,31} as well as in the nitration of tyrosine residues, an important oxidative post-translational modification occurring in proteins.^{32,33} The understanding and, possibly, the quantification of the role played by structure and external stimuli in the formation of phenoxy radicals can also be extremely useful to aid organic chemists in the design of simple bioinspired catalysts able to mimic nature in crucial processes, such as stereo- and chemoselective oxidations or energy transfer and storage.

EXPERIMENTAL SECTION

Materials. Spectroscopic grade acetonitrile was used in the kinetic experiments. Dicumyl peroxide, trifluoroacetic acid (TFA), and magnesium perchlorate (Mg(ClO₄)₂) were of the highest commercial quality available and were used as received. Phenols **2** and **3** were available from a previous work.⁹ Phenol **1** was prepared by the Betti reaction of phenol with paraformaldehyde and piperidine, according to a previously described procedure.³⁴ Paraformaldehyde (319 mg, 10.63 mmol) was dissolved in MeOH (1.5 mL) containing NaOH (2 mg); to this solution was added piperidine (905 mg, 10.63 mmol) in 0.5 mL of MeOH at 10 °C in 5 min, and after the mixture was warmed to room temperature, phenol (1000 mg, 10.63 mmol) was added in portions. The reaction mixture was heated to reflux with stirring for 17 h and then cooled to room temperature, diluted with EtOAc (100 mL), and washed with saturated NH₄Cl (100 mL). The organic phase was extracted with a HCl 1 M solution (200 mL), and the aqueous phase was basified with a solution of 10 M NaOH until pH 8 and extracted with EtOAc (2 \times 100 mL). The combined organic phases were dried over anhydrous Na₂SO₄, filtered, and concentrated under vacuum to obtain the desired product as a pale yellow oil (609 mg, 30% yield), identified by ¹H and ¹³C NMR (Supporting Information, Figures S17 and S18).

N-Benzylpiperidine was prepared by reductive amination of benzaldehyde with piperidine according to a previously described procedure.³⁵ In a round-bottomed flask containing benzaldehyde (0.658 g, 5.9 mmol) in distilled 1,2-dichloroethane (20 mL) was added piperidine (0.500 g, 5.9 mmol). Then, sodium triacetoxyborohydride (1.852 g, 8.3 mmol) was added in small portions and the reaction mixture was stirred at room temperature overnight. After 20 h the mixture was diluted with 80 mL of dichloromethane, and the organic phase was washed with a saturated solution of NaHCO₃ (3 \times 100 mL), dried over anhydrous Na₂SO₄, filtered, and concentrated under vacuum. The crude material was purified by washing the organic phase with a HCl 0.1 M solution (3 \times 50 mL); the aqueous layer was basified to pH 10 with a 1 M solution of NaOH and then extracted with DCM (3 \times 50 mL). The organic phases were recollected, dried over anhydrous Na₂SO₄, filtered, and concentrated under vacuum to obtain the desired product as a yellow oil (413 mg, 40% yield), identified by ¹H NMR (Supporting Information, Figure S19).

The occurrence of a strong intramolecular O–H...N hydrogen bond in **1** is confirmed by the large downfield shift exhibited by the phenolic proton in the ¹H NMR spectrum (10.4 ppm as compared to the usual 5–7 ppm value; see the Supporting Information).^{5a} The intramolecularly hydrogen bonded nature of **2** has been previously established.⁹

Laser Flash Photolysis Studies. LFP experiments were carried out with a laser kinetic spectrometer using the third harmonic (355 nm) of a Q-switched Nd:YAG laser, delivering 8 ns pulses. The laser energy was adjusted to $\leq 10 \text{ mJ/pulse}$ by the use of the appropriate filter. A 3.5 mL Suprasil quartz cell (10 mm \times 10 mm) was used in all experiments. Argon- or oxygen-saturated acetonitrile solutions of dicumyl peroxide (1.0 M) were employed. All of the experiments were carried out at $T = 25 \pm 0.5 \text{ }^\circ\text{C}$ with magnetic stirring. The observed rate constants (k_{obs}) were obtained by averaging two to five individual values and were reproducible to within 5%.

Second-order rate constants for the reactions of the cumyloxy radical with the different substrates were obtained from the slopes of the k_{obs} (measured following the decay of the cumyloxy radical visible absorption band at 490–540 nm) vs [substrate] plots. In the experiments carried out in the presence of TFA or $\text{Mg}(\text{ClO}_4)_2$, care was taken in order to keep the concentration of these compounds constant throughout the experiment. Fresh solutions were used for every substrate concentration.

■ ASSOCIATED CONTENT

■ Supporting Information

Figures giving time-resolved spectra and plots of k_{obs} vs substrate concentration for the reactions of CumO^\bullet and NMR spectra of phenol **1** and of *N*-benzylpiperidine. This material is available free of charge via the Internet at <http://pubs.acs.org>.

■ AUTHOR INFORMATION

Corresponding Authors

*E-mail for M.S.: michela.salamone@uniroma2.it.

*E-mail for M.B.: bietti@uniroma2.it.

Notes

The authors declare no competing financial interest.

■ ACKNOWLEDGMENTS

Financial support from the Ministero dell'Istruzione dell'Università e della Ricerca (MIUR), PRIN 2010-2011, project 2010PFLRJR (PROxi) is gratefully acknowledged. We thank Prof. Lorenzo Stella for the use of LFP equipment and Dr. Federica Ceccherini for the preparation of *N*-benzylpiperidine.

■ REFERENCES

- (1) Weinberg, D. R.; Gagliardi, C. J.; Hull, J. F.; Fecenko Murphy, C.; Kent, C. A.; Westlake, B. C.; Paul, A.; Ess, D. H.; Granville McCafferty, D.; Meyer, T. J. *Chem. Rev.* **2012**, *112*, 4016–4093.
- (2) (a) Dempsey, J. L.; Winkler, J. R.; Gray, H. B. *Chem. Rev.* **2010**, *110*, 7024–7039. (b) Kumar, A.; Sevilla, M. D. *Chem. Rev.* **2010**, *110*, 7002–7023. (c) Warren, J. J.; Tronic, T. A.; Mayer, J. M. *Chem. Rev.* **2010**, *110*, 6961–7001. (d) Hammes-Schiffer, S.; Stuchebrukhov, A. A. *Chem. Rev.* **2010**, *110*, 6939–6960. (e) Costentin, C.; Robert, M.; Savéant, J.-M. *Chem. Rev.* **2010**, *110*, PR1–PR40.
- (3) Mayer, J. M. *Acc. Chem. Res.* **2011**, *44*, 36–46.
- (4) (a) Styring, S.; Sjöholm, J.; Mamedov, F. *Biochim. Biophys. Acta* **2012**, *1817*, 76–87. (b) Barry, B. A.; Chen, J.; Keough, J.; Jensen, D.; Offenbacher, A.; Pagba, C. J. *Phys. Chem. Lett.* **2012**, *3*, 543–554. (c) Meyer, T. J.; Huynh, M. H. V.; Thorp, H. H. *Angew. Chem., Int. Ed.* **2007**, *46*, 5284–5304. (d) McEvoy, J. P.; Brudvig, G. W. *Chem. Rev.* **2006**, *106*, 4455–4483.
- (5) (a) Megiatto, J. D., Jr.; Méndez-Hernández, D. D.; Tejeda-Ferrari, M. E.; Teillout, A.-L.; Llansola-Portolés, M. J.; Kodis, G.; Poluëtkov, O. G.; Rajh, T.; Mujica, V.; Groy, T. L.; Gust, D.; Moore, T. A.; Moore, A. L. *Nat. Chem.* **2014**, *6*, 423–428. (b) Megiatto, J. D., Jr.; Antoniuk-Pablant, A.; Sherman, B. D.; Kodis, G.; Gervald, M.; Moore, T. A.; Moore, A. L.; Gust, D. *Proc. Natl. Acad. Sci. U.S.A.* **2012**, *109*, 15578–15583. (c) Moore, G. F.; Hambourger, M.; Kodis, G.; Michl, W.; Gust, D.; Moore, T. A.; Moore, A. L. *J. Phys. Chem. B* **2010**, *114*, 14450–14457. (d) Moore, G. F.; Hambourger, M.; Gervald, M.; Poluëtkov, O. G.; Rajh, T.; Gust, D.; Moore, T. A.; Moore, A. L. *J. Am. Chem. Soc.* **2008**, *130*, 10466–10467.
- (6) (a) Markle, T. F.; Tronic, T. A.; DiPasquale, A. G.; Kaminsky, W.; Mayer, J. M. *J. Phys. Chem. B* **2012**, *116*, 12249–12259. (b) Schrauben, J. N.; Cattaneo, M.; Day, T. C.; Tenderholt, A. L.; Mayer, J. M. *J. Am. Chem. Soc.* **2012**, *134*, 16635–16645. (c) Markle, T. F.; Rhile, I. J.; Mayer, J. M. *J. Am. Chem. Soc.* **2011**, *133*, 17341–17352. (d) Markle, T. F.; Mayer, J. M. *Angew. Chem., Int. Ed.* **2008**, *47*, 738–740. (e) Rhile, I. J.; Markle, T. F.; Nagao, H.; DiPasquale, A. G.; Lam, O. P.; Lockwood, M. A.; Rotter, K.; Mayer, J. M. *J. Am. Chem. Soc.* **2006**, *128*, 6075–6088.
- (7) (a) Zhang, M.-T.; Irebo, T.; Johansson, O.; Hammarström, L. *J. Am. Chem. Soc.* **2011**, *133*, 13224–13227. (b) Hammarström, L.; Styring, S. *Energy Environ. Sci.* **2011**, *4*, 2379–2388. (c) Irebo, T.; Johansson, O.; Hammarström, L. *J. Am. Chem. Soc.* **2008**, *130*, 9194–9195. (d) Sjödin, M.; Irebo, T.; Utas, J. E.; Lind, J.; Merényi, G.; Åkermar, B.; Hammarström, L. *J. Am. Chem. Soc.* **2006**, *128*, 13076–13083.
- (8) (a) Bonin, J.; Costentin, C.; Robert, M.; Savéant, J.-M.; Tard, C. *Acc. Chem. Res.* **2012**, *45*, 372–381. (b) Costentin, C.; Robert, M.; Savéant, J.-M.; Tard, C. *Angew. Chem., Int. Ed.* **2010**, *49*, 3803–3806. (c) Costentin, C.; Robert, M.; Savéant, J.-M. *Phys. Chem. Chem. Phys.* **2010**, *12*, 11179–11190. (d) Costentin, C.; Robert, M.; Savéant, J.-M. *J. Am. Chem. Soc.* **2007**, *129*, 9953–9963. (e) Costentin, C.; Robert, M.; Savéant, J.-M. *J. Am. Chem. Soc.* **2006**, *128*, 4552–4553.
- (9) Amorati, R.; Menichetti, S.; Viglianisi, C.; Foti, M. C. *Chem. Commun.* **2012**, *48*, 11904–11906.
- (10) For a comparison between the reactivity of alkoxy and peroxy radicals in HAT reactions from the α -C–H bonds of alkylamines, see for example: Griller, D.; Howard, J. A.; Marriott, P. R.; Scaiano, J. C. *J. Am. Chem. Soc.* **1981**, *103*, 619–623.
- (11) For a comparison between the reactivity of alkoxy and peroxy radicals in HAT reactions from the O–H group of phenols see for example: (a) Jha, M.; Pratt, D. A. *Chem. Commun.* **2008**, 1252–1254. (b) Snelgrove, D. W.; Luszyk, J.; Banks, J. T.; Mulder, P.; Ingold, K. U. *J. Am. Chem. Soc.* **2001**, *123*, 469–477.
- (12) Baciocchi, E.; Biatti, M.; Salamone, M.; Steenken, S. *J. Org. Chem.* **2002**, *67*, 2266–2270.
- (13) Avila, D. V.; Ingold, K. U.; Di Nardo, A. A.; Zerbetto, F.; Zgierski, M. Z.; Luszyk, J. *J. Am. Chem. Soc.* **1995**, *117*, 2711–2718.
- (14) (a) Biatti, M.; DiLabio, G. A.; Lanzalunga, O.; Salamone, M. J. *Org. Chem.* **2010**, *75*, 5875–5881. (b) Donkers, R. L.; Maran, F.; Wayner, D. D. M.; Workentin, M. S. *J. Am. Chem. Soc.* **1999**, *121*, 7239–7248.
- (15) Salamone, M.; DiLabio, G. A.; Biatti, M. *J. Am. Chem. Soc.* **2011**, *133*, 16625–16634.
- (16) Salamone, M.; Giammarioli, I.; Biatti, M. *Chem. Sci.* **2013**, *4*, 3255–3262.
- (17) Salamone, M.; Mangiacapra, L.; DiLabio, G. A.; Biatti, M. *J. Am. Chem. Soc.* **2013**, *135*, 415–423.
- (18) Avila, D. V.; Brown, C. E.; Ingold, K. U.; Luszyk, J. *J. Am. Chem. Soc.* **1993**, *115*, 466–470.
- (19) Scaiano, J. C. *J. Phys. Chem.* **1981**, *85*, 2851–2855.
- (20) Maillard, B.; Ingold, K. U.; Scaiano, J. C. *J. Am. Chem. Soc.* **1983**, *105*, 5095–5099.
- (21) Lalevée, J.; Allonas, X.; Fouassier, J.-P.; Ingold, K. U. *J. Org. Chem.* **2008**, *73*, 6489–6496.
- (22) (a) Biatti, M.; Salamone, M.; DiLabio, G. A.; Jockusch, S.; Turro, N. J. *J. Org. Chem.* **2012**, *77*, 1267–1272. (b) Biatti, M.; Calcagni, A.; Salamone, M. J. *Org. Chem.* **2010**, *75*, 4514–4520.
- (23) Das, P. K.; Encinas, M. V.; Steenken, S.; Scaiano, J. C. *J. Am. Chem. Soc.* **1981**, *103*, 4162–4166.
- (24) Abraham, M. H.; Grellier, P. L.; Prior, D. V.; Duce, P. P.; Morris, J. J.; Taylor, P. J. *J. Chem. Soc., Perkin Trans. 2* **1989**, 699–711.
- (25) Biatti, M.; Salamone, M. *Org. Lett.* **2010**, *12*, 3654–3657.
- (26) Nakanishi, I.; Kawashima, T.; Ohkubo, K.; Waki, T.; Uto, Y.; Kamada, T.; Ozawa, T.; Matsumoto, K.; Fukuzumi, S. *Chem. Commun.* **2014**, *50*, 814–816.
- (27) In Table 2 of the work cited in ref 9, the reduction potential of dpph^\bullet in acetonitrile solution should be read as 0.48 V/NHE instead of 0.69 V/NHE.
- (28) (a) Lucarini, M.; Pedulli, G. F. *Chem. Soc. Rev.* **2010**, *39*, 2106–2119. (b) Wright, J. S.; Johnson, E. R.; DiLabio, G. A. *J. Am. Chem. Soc.* **2001**, *123*, 1173–1183.
- (29) An analogous behavior (no increase in k_{obs} up to $[\text{Mg}(\text{ClO}_4)_2]/[\text{substrate}] = 1.5$) has been observed when the reactions between CumO^\bullet and other tertiary alkylamines have been carried out in the

presence of $\text{Mg}(\text{ClO}_4)_2$.¹⁷ At present we do not have a clear explanation for this peculiar stoichiometry.

- (30) Nova, A.; Balcells, D. *Chem. Commun.* **2014**, 50, 614–616.
- (31) (a) Minnihan, E. C.; Nocera, D. G.; Stubbe, J. *Acc. Chem. Res.* **2013**, 46, 2524–2535. (b) Stubbe, J.; van der Donk, W. A. *Chem. Rev.* **1998**, 98, 705–762.
- (32) Radi, R. *Acc. Chem. Res.* **2013**, 46, 550–559.
- (33) Feeney, M. B.; Schöneich, C. *Antioxid. Redox Signaling* **2012**, 17, 1571–1579.
- (34) Ramalingam, K.; Raju, N.; Nanjappan, P.; Linder, K. E.; Pirro, J.; Zeng, W.; Rumsey, W.; Nowotnik, D. P.; Nunn, A. D. *J. Med. Chem.* **1994**, 37, 4155–4163.
- (35) Addis, D.; Beller, M.; Das, S.; Junge, K.; Zhou, S. *Angew. Chem., Int. Ed.* **2009**, 48, 9507–9510.